Clays and Clay Minerals, Vol. 60, No. 3, 240–253, 2012.

CLAY MINERALOGY OF THE ZHADA SEDIMENTS: EVIDENCE FOR CLIMATIC AND TECTONIC EVOLUTION SINCE ~9 Ma IN ZHADA, SOUTHWESTERN TIBET

HANLIE HONG[1,2]*, CHAOWEN WANG[2], KEFENG ZENG[2], KEXIN ZHANG[1,2], KE YIN[2], AND ZHAOHUI LI[3]

[1] State Key Laboratory of Biogeology and Environmental Geology, China University of Geosciences, Wuhan, Hubei, 430074, P. R. China
[2] Faculty of Earth Sciences, China University of Geosciences, Wuhan, Hubei, 430074, P. R. China
[3] Geosciences Department, University of Wisconsin-Parkside, Kenosha, WI 53141-2000, USA

Abstract—The clay mineralogy of the Zhada sediments was investigated, using X-ray diffraction and scanning electron microscopy, to obtain a better understanding of climatic change and uplift of the Himalayas in the Zhada region of Tibet. The sediments of Zhada basin in the late Miocene to Pliocene consist of lacustrine and fluvial deposits >800 m thick and can be subdivided into five clay assemblage zones based on their clay-mineral composition. The upward zonation is as follows: (1) smectite-kaolinite; (2) illite-chlorite; (3) chlorite-illite-kaolinite; (4) illite-chlorite; and (5) smectite, illite, and kaolinite. The ratio of chlorite + illite to kaolinite + smectite (Ch+I/K+S) and the Kübler index indicate a warm and humid climate from 9.5 to 8.4 Ma, a cold and dry climate from 8.4 to 7.2 Ma, a warm and seasonal arid climate from 7.2 to 4.5 Ma, a cool and humid climate from 4.5 to 3.6 Ma, and a warm and seasonally humid climate from 3.6 to 3.0 Ma. Intense fluctuations in the Kübler index and in the quantities of evaporite minerals dolomite, aragonite, and gypsum, during the period 7.2−4.5 Ma suggest strong climatic fluctuations between humid and seasonally humid conditions in the Zhada basin. Rapid uplift around the Zhada basin occurred at 8.4 and 3.6 Ma, with sharp subsidence at 7.2 and 4.5 Ma. Evolution of the climate at Zhada showed a different model from that of global climate change, and tectonics-led climate change was the major contributor to climate evolution in the area.

Key Words—Kübler Index, Paleoclimate, Tibetan Plateau, Uplift, Zhada Basin.

INTRODUCTION

The Zhada basin is located at ~80ºE between the Himalayan and Transhimalayan Ranges to the south and north, and the Gurla Mandhata and Leo Pargil domes to the east and west, respectively. The basin stretches from the northwest to the southeast and is ~140 km long × ~50 km wide. The current elevation of the basin ranges from 4000 to 4500 m. The basin currently lies in the hinterland of the Himalayan fold-thrust belt and developed on a regionally extensive thrust system known to be active in the Middle Miocene (Figure 1). Sediments began to accumulate in response to the Middle/Late Miocene uplift of the Gurla Mandhata and Leo Pargil domes in the east and west, respectively (Murphy *et al*., 2002; Thiede *et al*., 2006). The Zhada sediments are of lacustrine and fluvial facies containing abundant *Hipparion*, gastropoda, ostracoda, and sporopollen (Li and Zhou, 2001), and the estimated age of these deposits have varied in the ranges 7−1 Ma (Qian, 1999), 9.5−2.6 Ma (Wang *et al*., 2008), and ~9−1 Ma (Saylor *et al*., 2009).

The Zhada sediments were derived from the uplifted mountains surrounding the basin and, therefore, document the climatic and environmental changes associated with the regional tectonics in the southwestern Tibetan Plateau (Kempf *et al*., 2009). Little work has been done on the climatic significance of the sediments (Saylor *et al*., 2010a). Sedimentary-facies and sporopollen-assemblage studies have indicated a generally cooling trend with several obvious fluctuations between warm/humid and cold/dry climate conditions during the period in question (9.5−3.0 Ma) (Zhu *et al*., 2007). Based on sedimentological, petrographic, and paleoecological investigations, the Zhada sequence was suggested (Kempf *et al*., 2009) to have been caused by a combination of tectonic basin subsidence and intensified summer monsoon precipitation. The thick and massive conglomerate beds in the upper part of the section reflected the onset of northern hemisphere glaciation and strengthening of winter monsoon. From sequence stratigraphy, isotope stratigraphy, and lithostratigraphy studies, Saylor *et al*. (2010a) suggested that climate evolution in Zhada basin was characterized by distinct dry/wet cycles which were attributed to both the global and the regional tectonics-led climate changes.

Variation in the clay minerals contained in sediments and sedimentary rocks may have resulted from modifications to detrital sediments related to tectonically controlled changes in sediment source, or from changes in the intensity of weathering or variations in depositional conditions depending on climatic conditions and sea level (Schieber, 1986; Chamley, 1989; Fagel *et al*., 1994; 2003). Clay minerals have been used widely as

* E-mail address of corresponding author:
honghl8311@yahoo.com.cn
DOI: 10.1346/CCMN.2012.0600302

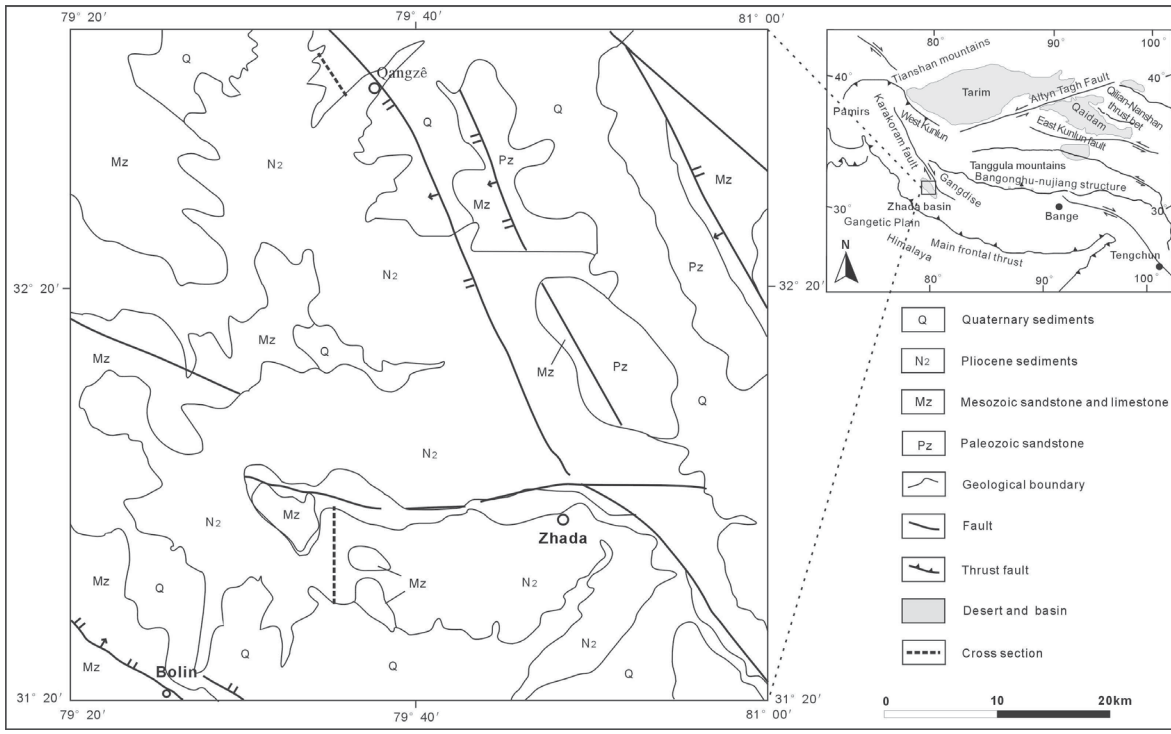

Figure 1. Location and regional geology of the Zhada basin and the sampling site (adapted from Zhu *et al*., 2007).

proxies for climate reconstruction in marine and lacustrine environments (*e.g*. Chamley, 1989; Thiry, 2000). Study of the clay minerals of basin sediments can provide evidence of climatic and environmental changes and, in particular, of topographic changes related to uplift in the area (Thiry, 2000; Hong *et al*., 2007, 2010). Previous studies of the Zhada sediments, however, have focused mainly on chronology, sedimentology, and sporopollen assemblages; clay-mineral investigations of the sediments have not been undertaken. Climatic and environmental changes in the area are still poorly understood. In the present study the focus was on determining changes in clay-mineral indices of the Zhada sediments, using X-ray diffraction (XRD) and scanning electron microscopy (SEM) combined with the sedimentary-facies investigation of the sediments, to obtain a better understanding of climatic and environmental evolution and uplift of the Himalayas in the Zhada basin, western Tibetan Plateau in the last 9 Ma.

GEOLOGICAL SETTINGS AND SAMPLING

The Zhada basin deposits lie unconformably on the Mesozoic limestone and low-grade metamorphic sandstones, with a total thickness of ~800 m, consisting of 174 lithological layers, and they can be subdivided roughly into three sections. The lower section comprises a generally upward-fining succession of cycles. It consists mainly of sandstones and pebble- to cobble-sized conglomerates, with thin, fine-grained, laminated siltstone and mudstone interbeds, containing abundant mammal, gastropod, and plant fossils. Sandstones of this section, which is ~200 m thick, are generally cross-bedded and the section has been interpreted as a fluvial deposit (Zhu *et al*., 2007; Saylor *et al*., 2009).

Unlike the lower section, the middle section comprises a generally upward-coarsening succession of cycles and consists of mudstones and marls interbedded with sandstones and conglomerates, ~250 m thick. In an individual cycle, profundal lacustrine mudstone occurs in the lower part, while deltaic and wave-worked sandstone and conglomerate are found in the upper part. In general, the coarse lithological layers show upward thinning while the fine-grained lithological layers show upward thickening. The mudstone is devoid of macrofossils, while the sandstone often has well preserved, robust gastropod shells. The upward coarsening succession of cycles was considered as progradational lacustrine sequences by Zhu *et al*. (2007) and Saylor *et al*. (2009).

The upper section comprises mainly conglomerate and sandstone, and thin mudstone and marl interbeds. It continues the upward-coarsening progression displayed in the middle portion but becomes much coarser, and the lithological layers exhibit an upward-thickening trend. Oblique-bedded texture was commonly observed in the conglomerates and sandstones. This portion is ~350 m thick and is interpreted as lake-margin, alluvial-fan, and

fan-delta deposits, reflecting a retrogradational lacustrine deposit. Conglomerates commonly occur within the section, especially in the lower and upper sections, reflecting the multi-staged uplift of the surrounding mountains, and marls and mudstones in the sediments are indicative of periods of stable lacustrine environment. The general grain size and lithofacies cycles of the Zhada sequence suggest the complete evolution of a lacustrine basin from the expanding to shrinking phase.

The Zhada section studied included two continuous profiles. The lower Zhada sequence is located near Bolin village, ~20 km southwest of Zhada city, and the upper Zhada sequence is located near Qangzê town (Figure 1). The samples were collected from the same sections as studied by Wang *et al*. (2008) and so the same age range of 9.5−2.6 Ma was adopted. The Zhada basin shrank and has not received sediment since 2.6 Ma. For the present study, the samples were collected according to their lithological characteristics from ~1 m depth, to ensure sample freshness. The sampling intervals in the Zhada sequence were usually ~1−4 m in siltstone, mudstone, and marl layers, and were up to ~8 m in thick conglomerate and sandstone. The thick and massive conglomerate beds in the upper part of the section were not suitable for clay mineralogical study and so no samples were collected. A total of 174 samples was collected, representing the depth range of 0 to 720 m from the basin floor and an age range of 9.5−3.0 Ma.

EXPERIMENTAL METHODS

XRD analysis

Bulk samples (~200 g each) were air dried and then crushed and ground to powder using a mortar and pestle. The clay fraction (<2 μm) was obtained by the sedimentation method as described by Jackson (1978). The oriented clay fraction was prepared by pipetting the clay suspension carefully onto a glass slide. After scanning, the air-dried samples were treated with ethylene glycol vapor at ~65ºC for 3 h and then rescanned. The XRD measurement of the samples was carried out on a Rigaku D/Max-IIIA diffractometer with Ni-filtered CuKα radiation (35 kV, 35 mA) and the slit conditions were: 1º divergence slit, 1º anti-scatter slit, and 0.3 mm receiving slit. The XRD patterns were collected from 3 to 65º2θ at a scan rate of 4º2θ/min.

The non-clay minerals calcite, dolomite, aragonite, quartz, gypsum, orthoclase, and plagioclase were identified by their characteristic peaks at 3.03, 2.89, 3.39, 3.34, 7.60, 3.23, and 3.18 Å, respectively. Their relative abundances in the bulk samples were determined using a reference intensity method (Hillier, 2000) with corundum as the internal standard.

The relative proportions of clay minerals in the clay fraction were estimated semi-quantitatively using peak heights, as described by Biscaye (1965). The peak intensities of the characteristic reflections were measured from the XRD patterns of the ethylene glycol-saturated clay samples, and the relative abundances of clay minerals were determined using the formula: $4 \times$ I (illite-10 Å) + I (smectite-17 Å) + $2 \times$ I (kaolinite, chlorite) = 100%. The abundances of kaolinite and chlorite were further calculated by the intensities of the 3.58 Å reflection of kaolinite and the 3.52 Å reflection of chlorite. The illite crystallinity was determined using the Kübler index, which was expressed as the full width at half-height of the 001 reflection of illite in the XRD pattern of the air-dried clay fractions. The greater the Kübler index value, the lower the illite crystallinity.

SEM analysis

Examination by SEM was undertaken to determine the effect of diagenesis on the clay mineralogy and the origin of the carbonates (*e.g*. calcite, aragonite, and dolomite). Representative samples were selected from the sediments according to the XRD-determined clay-mineral assemblages and Kübler indexes. Small blocks of the selected rock samples were cut to ~1 cm in diameter and were then coated with platinum. The SEM examinations were carried out using a JSM-5610 scanning electron microscope with an energy-dispersive spectrometer (EDS) system. The diagenesis of the sediments was determined based largely on the texture of the clay minerals, and the origins of carbonates and gypsum were based on their crystal behaviors.

RESULTS

Mineral composition of the sediments

The XRD results of the bulk samples and of the <2 μm clay fractions showed that non-clay minerals are mainly quartz, calcite, feldspars, dolomite, and minor gypsum and aragonite, while the clay minerals are mainly illite, smectite, kaolinite, and chlorite (Figures 2, 3). The abundances of non-clay minerals vary greatly along the section (Figure 4). Calcite cement is abundant in the 9.5−3.6 Ma sediments, minor dolomite is present in the 7.2−4.5 and 3.6−3.0 Ma sediments, aragonite occurs occasionally in the 7.2−4.5 Ma sediments, and gypsum occurs occasionally in the 9.5−3.6 Ma sediments.

Illite, smectite, and kaolinite are ubiquitous throughout the Zhada sediments, and their relative proportions vary considerably along the profile (Figure 5). Illite is the most abundant clay mineral in the sediments, usually <45% in the 9.5−8.4 Ma sediments, increasing to 45−81% in the middle interval (8.4−3.6 Ma), and decreasing sharply at 3.6 Ma. Chlorite is typically <20% in the lower section of 9.5−8.4 Ma and is absent from the upper section of 3.6−3.0 Ma except for one sample, while it increases to 20−40% in the middle section of 8.4−3.6 Ma. Smectite exhibits the opposite trend to chlorite and illite. It is abundant in the lower section (with typically 30−80%) and in the upper section

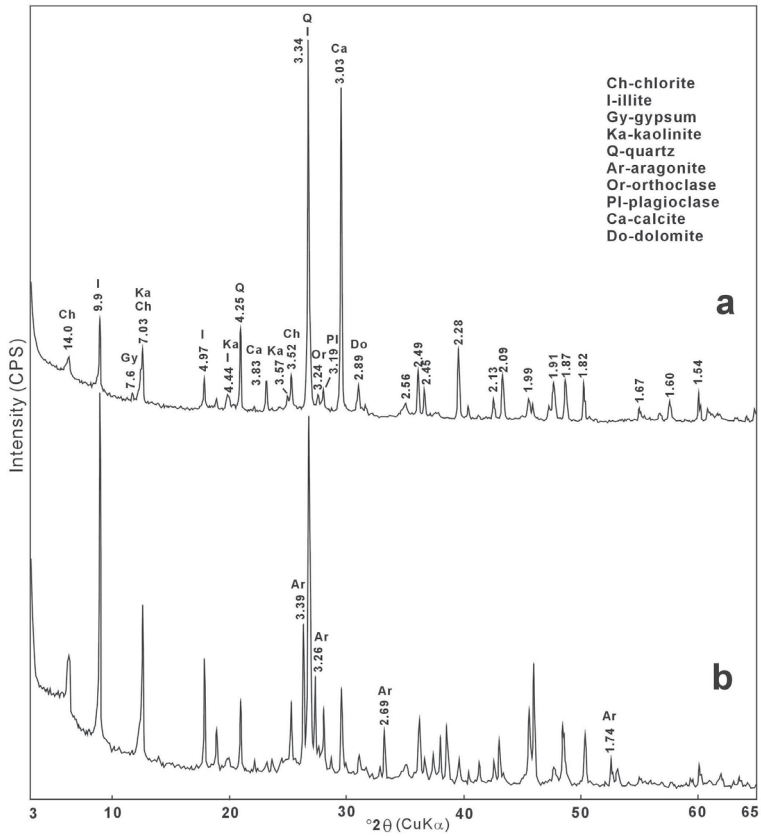

Figure 2. Representative XRD patterns of bulk samples showing the mineral components of the Zhada sediments.

(25−50%), while it is less abundant in the middle interval with a content of usually <10%.

The sum of illite and chlorite varies from 20 to 70% in the lower and upper intervals of 9.5−8.4 and 3.6−3.0 Ma, and it increases rapidly to 70−90% from ~8.4 to 3.6 Ma in the middle section. During the period 9.5−3.0 Ma, however, two sharp changes in the illite and chlorite contents occurred at 8.4 and 3.6 Ma, respectively. The Kübler index value is significantly larger in the periods 9.5−8.4 and 7.2−4.5 Ma, and is smaller in the stages 8.4−7.2 and 4.5−3.6 Ma.

The Zhada sediments can be subdivided into five clay mineral assemblages, according to the changes in relative contents of each clay mineral and in the Kübler index. The smaller interval 9.5−8.4 Ma contains mainly smectite and kaolinite, with less illite and chlorite, and the Kübler index value is moderately large. The middle interval with ages of 8.4−7.2 Ma and 4.5−3.6 Ma contains mainly illite and chlorite, with only trace smectite and kaolinite, and the Kübler index value is the smallest, while sediments of 7.2−4.5 Ma contain mainly illite, chlorite, and minor kaolinite, with a significantly greater Kübler index value. The upper interval of 3.6−3.0 Ma contains mainly smectite and kaolinite, with less illite and chlorite, and the Kübler index value is moderately low. In summary, the five clay-assemblage zones in the Zhada sediments are: (1) smectite-kaolinite, (2) illite-chlorite, (3) chlorite-illite-kaolinite, (4) illite-chlorite, and (5) smectite, illite, and kaolinite, respectively (Table 1, Figure 5). Rapid changes in the clay-mineral composition, ratio of chlorite + illite to kaolinite + smectite (Ch+I/K+S), and the Kübler index value occur at 8.4, 7.2, 4.5, and 3.6 Ma, respectively (Figure 5).

SEM analysis

The Zhada sediments have a loose texture and are poorly cemented. Clay particles usually occur in discrete clasts with angular and irregular outlines, which fill the interstitial space between larger detrital particles, and aggregates of clay particles usually exhibit the typical swirly texture indicating a detrital origin for the clay grains (Figure 6a).

The clay particles display anhedral morphology typical of detrital provenance. The clay flakes usually exhibit a bent shape with relatively smooth basal (001) planes, and their lateral surfaces are notably uneven, with irregular outlines or ragged edges. The lateral dimensions of the clay flakes are poorly defined, with particularly thin plates and well developed fissures, suggesting origin in detrital clasts. The size of basal-plane dimensions of clay flakes ranges mainly from 0.5

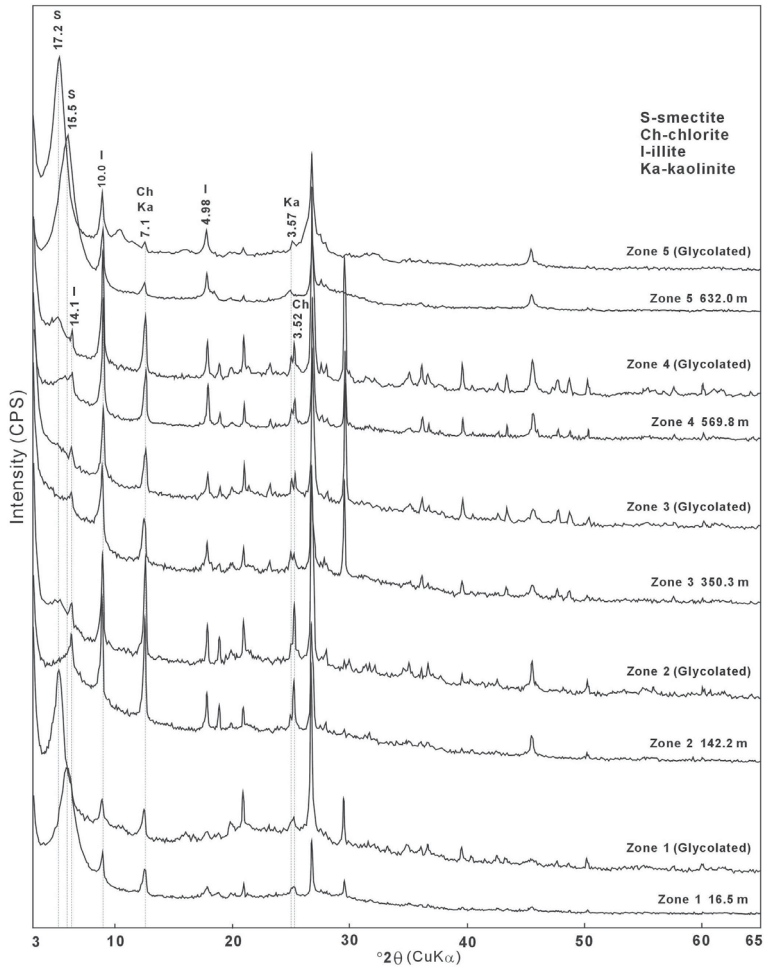

Figure 3. Representative XRD patterns of air-dried and glycolated clays of the sediments. Zone 1: smectite-kaolinite clay assemblage; Zone 2: illite-chlorite clay assemblage; Zone 3: chlorite-illite-kaolinite clay assemblage; Zone 4: illite-chlorite clay assemblage; and Zone 5: smectite, illite, and kaolinite clay assemblage. The 15 Å reflection of air-dried smectite expanded to 17.2 Å after glycol treatment.

to 4 μm, and the thickness is usually <0.3 μm. Mostly degraded outlines of platy kaolinite, flaky smectite, lathy illite, and platy chlorite crystals of the sediments are shown (Figure 6a–d). Analysis by EDS of irregular kaolinite plates yielded strong peaks for Si and Al, and smectite flakes were indicated by strong Si, moderate Al, and smaller Ca and Fe peaks (Figure 6a,b). The EDS spectra for the lathy illite are characterized by strong Si and Al and moderate K peaks, and chlorite plates by strong Si, moderate Al, and smaller Mg, Fe, and K peaks (Figure 6c,d).

Well developed rhombohedral crystals with smooth plane surfaces were also observed in the sediments, with chemical compositions (determined by EDS) mainly of Ca and of Ca and Mg (Figure 6e), suggesting that these are crystals of calcite and dolomite, respectively. The characteristic rhombohedral habit of calcite and dolomite in the sediments indicated deposition from solution instead of from a detrital source. Euhedral gypsum is present in the sediments and yielded strong Ca and S peaks (Figure 6f), indicating crystallization directly from solution (*i.e.* authigenetic origin).

DISCUSSION

Evidence for the detrital origin of the clay minerals

The Zhada basin sediments are ~800 m thick. They overly unconformably Mesozoic limestone and low-grade metamorphic sandstones. The XRD results for the Zhada sediments indicated that only discrete illite, chlorite, smectite, and kaolinite occur in the sediments, and mature R1 illite-rich mixed layers of possible diagenetic origin are absent from the deposits. Discrete minerals in the sediments, which are immature for oil-generation purposes, were predominantly of detrital origin and the characteristics of the clay minerals depend largely on the parent rocks (Lindgreen and Surlyk, 2000; Hong *et al*., 2007). Mixed-layer illite-

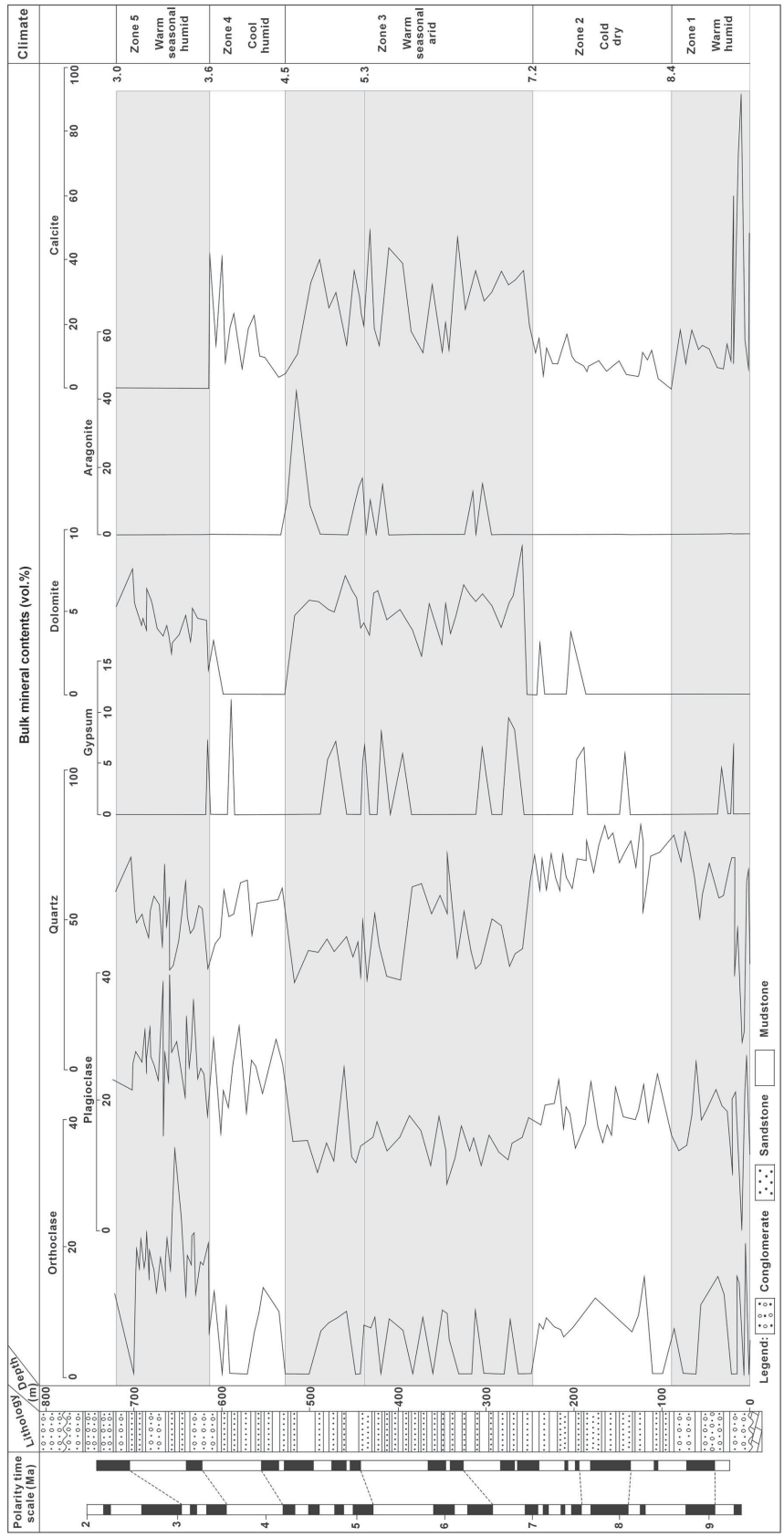

Figure 4. Changes in mineral content of the bulk sediments along the Zhada section.

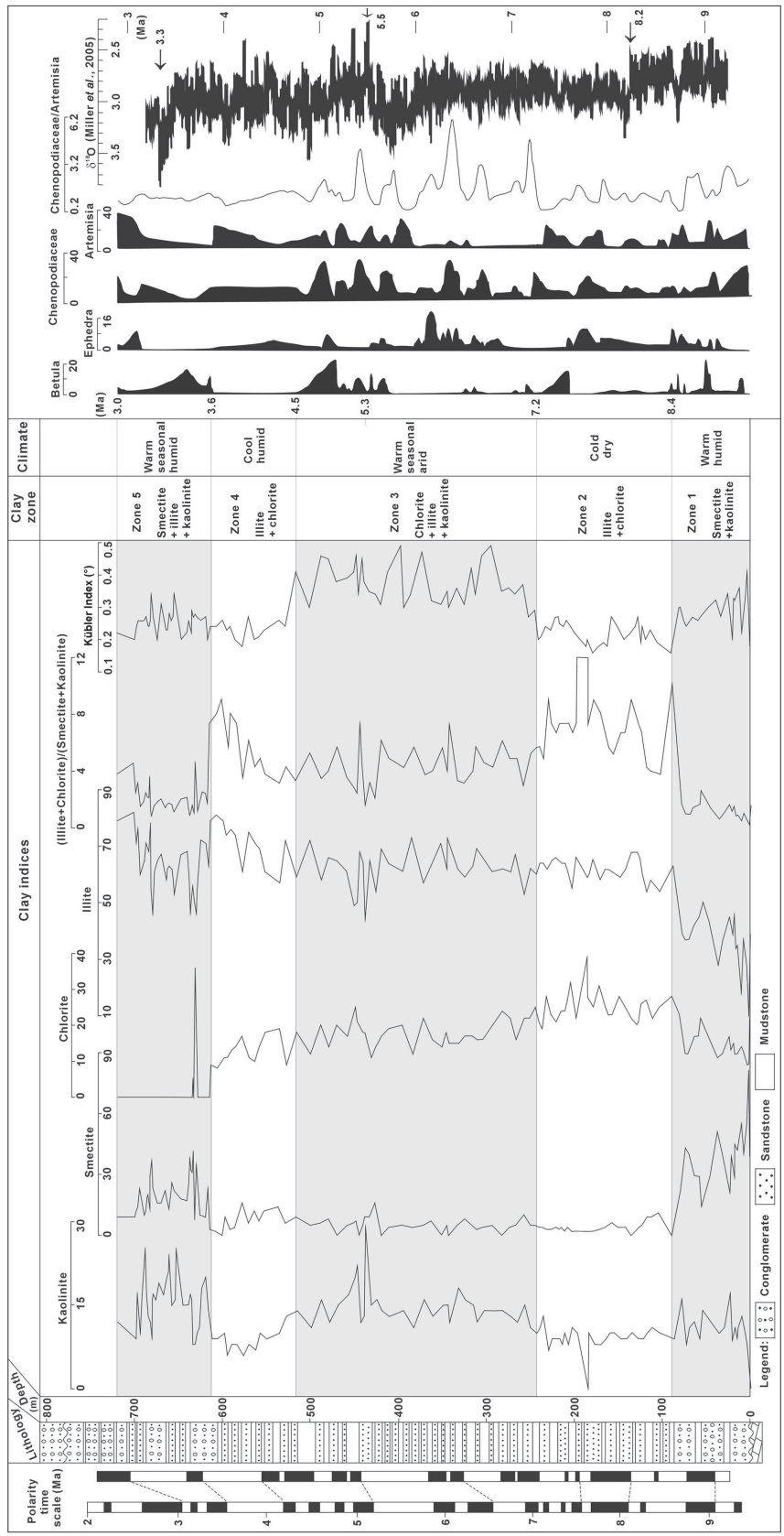

Figure 5. Relative proportions of clay minerals in the <2 μm fraction and clay indices of the Zhada sediments (illite crystallinity expressed in terms of the Kübler index; global $\delta^{18}O$ isotope record adapted from Miller *et al.* (2005); Sporopollen data adapted from Zhu *et al.* (2007)).

Table 1. Relative proportions of clay minerals in sediments of the five climate zones.

Clay zone	Relative content (vol.%)		Mean value (vol.%)	Age (Ma)	Climate
Zone 5	Smectite	8–41	20	3.6–3.0	Warm and seasonal humid
	Illite	46–82	63		
	Kaolinite	8–25	16		
	Chlorite	0–36	1		
Zone 4	Illite	57–81	72	4.5–3.6	Cool and humid
	Chlorite	8–19	13		
	Smectite	0–14	7		
	Kaolinite	6–13	8		
Zone 3	Illite	44–73	61	7.2–4.5	Warm and seasonal arid
	Chlorite	12–25	17		
	Kaolinite	11–29	14		
	Smectite	0–16	5		
Zone 2	Illite	20–68	58	8.4–7.2	Cold and dry
	Chlorite	13–32	24		
	Smectite	0–9	6		
	Kaolinite	0–11	8		
Zone 1	Smectite	14–81	39	9.5–8.4	Warm and humid
	Kaolinite	0–17	10		
	Illite	10–50	36		
	Chlorite	9–23	14		

smectite clays can be formed as intermediate products of the transformation from smectite to illite during diagenesis, and the transformation of illite-smectite often takes place at the temperature range of oil formation (Perry and Hower, 1970). Diagenesis should result in an increase in illite crystallinity with depth. Pure smectite occurs frequently at the top and at the bottom of the profile, however. Progressive burial diagenetic illitization of smectite is not indicated. The Kübler index value ranges from 0.15º to 0.50º, in good agreement with illite arising from anchimetamorphism rather than from diagenesis. Illite with smaller crystallinity index values is present in the lower interval, while in the upper interval the illite has greater crystallinity, indicating that variations in the illite crystallinity of the sediments must be due to different parent materials (Figure 5).

Diagenesis may also have resulted in changes in the clay morphology. The swirly texture of the clay aggregates and the discrete clay particles with angular and irregular outlines (Figure 6) are indicative of a detrital origin (Manju *et al.*, 2001). Therefore, the clay mineralogy of the Zhada sediments may well reflect the characteristics of the parent materials.

Zhada clays vs. parent-rock minerals

Sedimentary investigations of the remnant basins in the Tibetan Plateau showed that local tectonic uplift took place along the Tengchun-Bange-Zhada zone during the Paleocene–Eocene period, and erosion began in the Zhada area ~34 Ma ago (Zhang *et al.*, 2008). The expanded uplift zones of the Gangdise, Himalaya, Karakoram, and Kunlun blocks resulted in local uplift and the formation of a number of intermountain basins during Miocene–Pliocene time (Aitchison *et al.*, 2007). The Zhada basin was formed and sediments from the surrounding highlands began accumulating there ~9.5 Ma ago (Wang *et al*., 2008; Saylor *et al*., 2010b).

The bedrocks of the Zhada area are mainly Mesozoic limestones and low-grade metamorphic sandstones, containing mainly illite, chlorite, and minor kaolinite (Wang *et al*., 2008). In the Miocene–Pliocene, intense weathering and pedogenesis took place in the south Tibetan Plateau, and red to red-brown relic paleosols, consisting mainly of smectite, kaolinite, and illite, were formed (Huang *et al*., 1999; Huang and Wang, 2001). Changes in detrital mineral composition, the Kübler index value, and the relative abundance of clay minerals in the Zhada sediments may reflect erosion of various source rocks into the basin at different times.

Detrital feldspars and quartz displayed a similar trend in terms of their relative abundances (Figure 4). They are abundant in the period ~9.5–7.2 Ma (Zones 1 and 2), indicating that the Zhada sediments were derived from the same sources. Differences in the clay mineral assemblage and in the Kübler index value were observed, however, between Zone 1 (~9.5–8.4 Ma) and Zone 2 (8.4–7.2 Ma) (Figure 5). The greater Kübler index value was associated with larger smectite and kaolinite contents in Zone 1 and suggested that the clay mineralogy during the period ~9.5–8.4 Ma was pro-

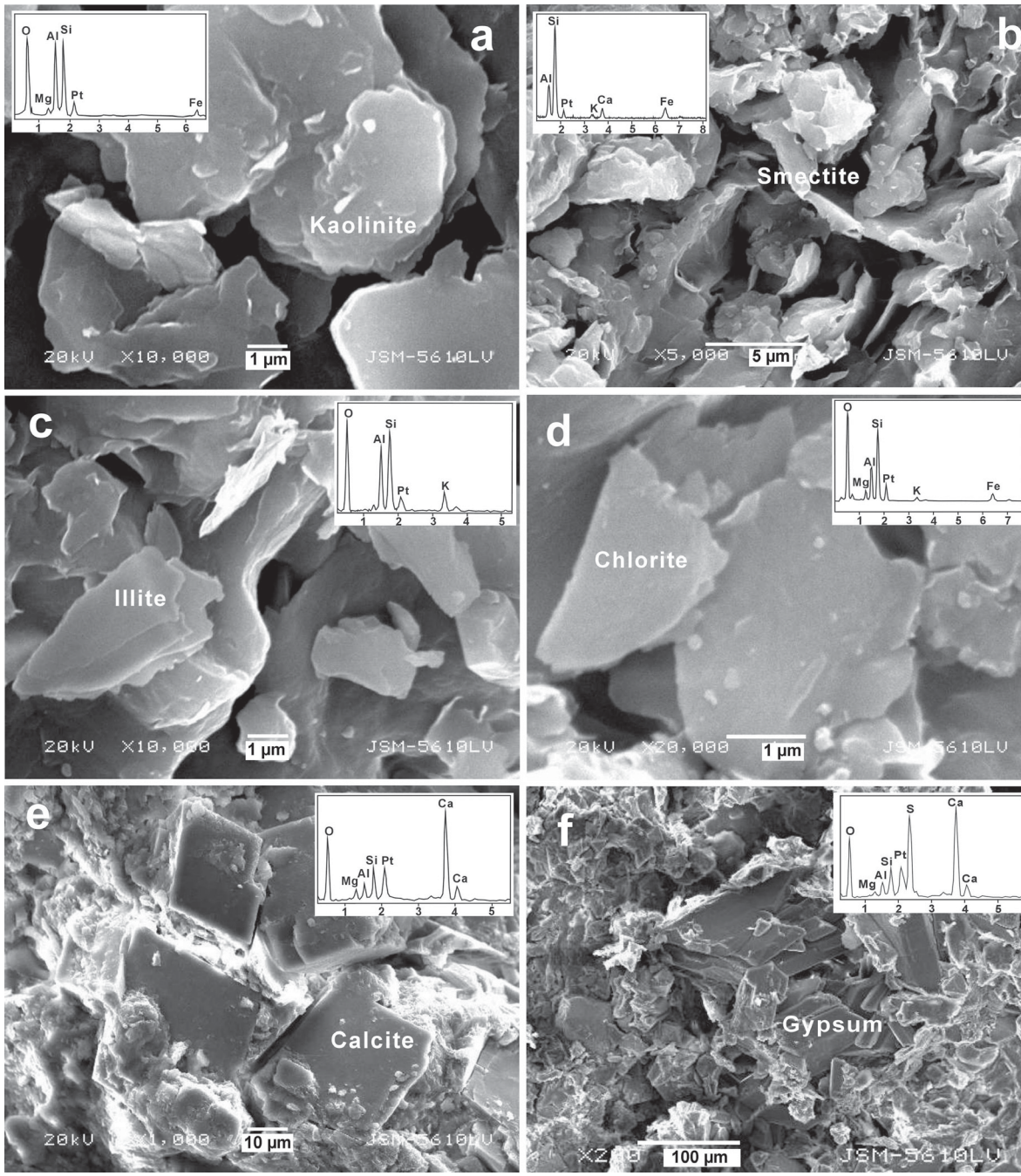

Figure 6. SEM images of the samples. (a) Swirl texture with face-to-face arrangement of detrital clay particles and clay-particle morphology of the Zhada sediments. Kaolinite crystals as thin pseudo-hexagonal plates with flat surfaces and irregular outlines. (b) Smectite, wavy in most cases, with bending and ragged edges. (c) Illite usually in lathy grains with irregular outlines. (d) Chlorite crystals exhibiting poorly developed thick plates with irregular outlines or ragged edges. (e) Euhedral, rhombohedronal carbonate crystals indicating deposition from solution. (f) Euhedral platy gypsum crystals suggesting an authigenic origin.

duced mainly by weathering. The abundance of feldspar and quartz decreased while that of carbonates increased in Zone 3 (7.2−4.5 Ma). Evidence from SEM suggested that carbonates in the sediments crystallized directly from solution (Figure 6e) and the occurrence of abundant calcite, dolomite, and aragonite in this period could, therefore, be attributed to climate conditions instead of erosion of the carbonate bedrocks. The larger Kübler index value probably resulted from intense hydrolysis of illite during weathering and sedimentary

processes. The (Ch+I)/(K+S) value was significantly smaller than that of Zone 2, together with increasing kaolinite abundance, indicating relatively strong pedogenesis during the episode. Thus, changes in mineral composition and clay mineralogy of the sediments (Zone 3) could be attributed to climate conditions rather than changes in erosion of source rock during the period. Detrital feldspar and quartz increased dramatically in Zone 4 (4.5−3.6 Ma), associated with the smaller Kübler index value and the larger (Ch+I)/(K+S) ratio, suggesting that erosion cut into deeper bedrocks than in the previous period. The increasing grain size of the sediments also indicated increasing erosion during this period (Saylor *et al*., 2009). Zone 5 (3.6−3.0 Ma) had a slightly larger Kübler index value but notably lower (Ch+I)/(K+S) ratio relative to Zone 4. The significant increase in kaolinite and smectite abundance reflects the increasing pedogenesis, and the total lack of chlorite and calcite in this zone seemed indicative of erosion of soils from weathering rather than erosion of the source rock of older horizons.

Mineral indicators of climatic conditions

Smectite forms in poorly drained, tropical to subtropical areas of low relief marked by flooding during humid seasons and substantial pore water in the soil during dry seasons. Kaolinite is one of the most common soil-derived clay minerals which can form rapidly within a time period of 50 y under tropical conditions (Gaucher, 1981; Hallam *et al.*, 1991), where abundant rainfall favored ionic transfer and pedogenic development (Millot, 1970; Chamley, 1989). Both kaolinite and smectite formed as a result of intense chemical weathering on land, and kaolinite and smectite are, therefore, considered as the end products of rock degradation in the hinterland and *in situ* weathering profiles (Chamley, 1989).

Illite is usually regarded as a little-altered detrital mineral derived from the existing bedrock or soil profile (Millot, 1970; Weaver, 1989). Chlorite occurs commonly in greenschist-grade metamorphic rocks and in sedimentary rocks. Chlorite is stable in cold regions marked by very low rates of weathering (Hallam *et al.*, 1991). It thus has an origin similar to illite in that physical weathering tends to allow chlorite to survive and even be concentrated in the erosion cycle (Madhavaraju *et al.*, 2002). In general, illite and chlorite are characteristic of cold regions and deserts marked by very low rates of chemical weathering and areas of steep relief where mechanical erosion interferes with soil formation (Chamley, 1989; Weaver, 1989; Robert and Kennett, 1994).

Unlike the burial diagenetic process, hydrolyzation of clay minerals in the weathering process will lead to a decrease in crystallinity. The crystallinity of illite is commonly used to differentiate cold-dry from warm-humid climate conditions (Singer, 1984). High rainfall and temperature are expected to be conducive to strong hydrolyzation of illite and result in lower illite crystallinity, while cold-dry climate conditions will favor the preservation of illite crystallinity. Thus, a change in the degree of weathering will produce materials of different clay-mineral assemblages and illite crystallinity. The variations in clay-mineral assemblage, the relative proportions of clay minerals, and illite crystallinity in the Zhada sediments are probably indicative of complex processes of mechanical erosion of unweathered bedrocks due to increasing relief by local tectonic uplift and chemical weathering under the local climatic conditions.

Evaporite minerals occur commonly in basin sediments. Dolomite is known to form in saline lakes in regions with arid climates, in association with biological activity (Van Lith *et al*., 2003; Solotchina *et al*., 2009), and aragonite is considered to form in warm-climate conditions (Anadón *et al*., 2002). Gypsum usually forms in closed basins when strong evaporation of surface waters takes place under extreme warm and arid climate conditions (Grosjean *et al*., 2001). Evaporite deposits from closed basins are sensitive to climate changes and have been used as a proxy for arid paleoclimatic conditions (Enzel *et al.*, 1999; Grosjean *et al.*, 2001).

Paleoclimatic evolution in the Zhada area

Illite and kaolinite were observed throughout the Zhada sediments, while smectite and chlorite are abundant, but occasionally absent from some intervals (Figure 5). The relative proportions of clay minerals exhibited significant variations in different layers along the Zhada profile. The abundant illite and chlorite in the Zhada sediments may reflect the steep relief of the region, and the elevated kaolinite and smectite contents in some sections suggest that a warm/humid climate was alternating with a cold/dry climate over the Late Miocene and Pliocene.

Changes in the relative amounts of clay minerals correlate with those of Kübler index values and (Ch+I)/(K+S) ratios (Figure 5). In Zone 1 (~9.5−8.4 Ma), the illite and chlorite contents as well as the (Ch+I)/(K+S) value were small, while the smectite and kaolinite contents and the Kübler index value were notably large, indicative of seasonally warm and wet climatic conditions. As the bulk minerals are mainly quartz, feldspar, and calcite, the large amounts of detrital quartz and feldspar suggest high water influx, and the large amounts of calcite and the occasional presence of gypsum also point to warm and wet climate conditions (Figures 4 and 5). Sporopollen analysis by Zhu *et al*. (2007) showed that chenopodiaceae, artemisia, ephedra, and betula are present to a significant extent in Zone 1 (Figure 5). The sporopollen assemblage and especially the large chenopodiaceae/artemisia value suggest warm and humid climate conditions, consistent with the clay mineralogical evidence. However, the gradual decrease of smectite and the gradual increase of illite and chlorite and Kübler index suggest a cooling trend during the period.

In the subsequent Zone 2 (8.4−7.2 Ma BP), the increasing abundances of illite and chlorite, the large (Ch+I)/(K+S) ratio, and the small Kübler index value suggest relatively cool and dry paleoclimate conditions with stronger physical erosion than in Zone 1. The amounts of bulk minerals, quartz and feldspar, present are notably quite large, and gypsum and dolomite occur sporadically in the sediments, which also suggest strong physical erosion under dry climate conditions. The cool and dry climate conditions in Zone 2 are supported by the presence of abundant ephedra and the smaller chenopodiaceae/artemisia value (Figure 5). Similar climatic changes in the period have been reported in areas near the Zhada basin. Paleobotanical evidence in the form of fossil leaves has indicated an environmental change from forest to grassland with fossil pollen at ~8−6.5 Ma in Nepal (Hoorn *et al*., 2000). Based on studies of both pollen and increasing pedogenic carbonates in the Thakkhola graben of Nepal, Garzione *et al*. (2003) suggested a particularly arid episode between 8 and ~7 Ma.

Kaolinite increased considerably but smectite decreased in Zone 3 (7.2–4.5 Ma BP). The Kübler index value is quite large (Figure 5), indicating notable climatic and environmental changes in the Zhada region after 7.2 Ma. Detrital quartz and feldspar decreased greatly, while calcite and dolomite were abundant. Aragonite and gypsum are mainly present in this period. These minerals suggest a much warmer climate relative to the previous stage; an unusually warm and seasonal arid climate over the period 7.2−4.5 Ma BP. This significant climatic change is consistent with the expansion of C_4 biomass (Saylor *et al*., 2009). Climate transition observed at 7.2 Ma in the Zhada region is in good agreement with climate changes elsewhere in the Himalaya (Flynn and Jacobs, 1982; France-Lanord and Derry, 1994; Quade *et al*., 1995; Garzione *et al*., 2000; Ojha *et al*., 2000; Wang *et al*., 2006). As shown in Figure 5, the Kübler index value shows considerable fluctuations, though it has a large value overall in the period, indicating fluctuations between warm/humid and warm/arid conditions, consistent with the results of Dettman *et al*. (2001) and Kempf *et al*. (2009). The presence of abundant ephedra and chenopodiaceae and the fluctuating but overall large chenopodiaceae/artemisia value also reflect an unusually warm and seasonal arid climate in the period (Figure 5). These climate patterns are similar to those of the Gyirong area in the period 6.7−5.5 Ma BP (Hong *et al*., 2010), which was probably caused by intensity variations of the Asian monsoon (An *et al*., 2001; Hu *et al*., 2005).

In Zone 4 (4.5−3.6 Ma), the Kübler index value decreases significantly while smectite and kaolinite are still present, though in trace amounts only. Illite shows an upward increase and chlorite the opposite trend. Detrital quartz and feldspar increase notably. Calcite is present in relatively large amounts, and gypsum occurs sporadically in the sediments. Aragonite and dolomite are absent from this zone, however. These are indicative of much cooler and more humid climate conditions during the period in comparison with the previous stage of 7.2−4.5 Ma, in good agreement with the absence of betula and the smaller chenopodiaceae/artemisia value.

In Zone 5 (3.6−3.0 Ma), the notable increase in smectite and kaolinite and the decrease in chlorite and illite, together with the slightly increasing Kübler index value and the significantly small (Ch+I)/(K+S) value, are indicative of warm and seasonal humid climate conditions during the episode. Detrital quartz and feldspar increased significantly, while aragonite, calcite, and gypsum were absent from the deposits, suggesting the dilution of the water, which also point to the warm and seasonal humid climate conditions. The warm and seasonal humid climate conditions in Zone 5 agree well with the relatively abundant betula and smaller chenopodiaceae/artemisia ratio.

Tectonic uplift in the Zhada area

In basin sediments of the Tibetan Plateau, clay mineral assemblages reflect the chemical weathering of the parent rocks linked to local climate changes as well as landscape and tectonic activity in association with the structural evolution of the blocks (Hong *et al*., 2007; 2010). The differential tectonic uplift in the Tibet Plateau would have produced steep relief and increased the mechanical erosion in the area, and when the uplift reached a certain elevation, it may also have blocked winds bearing tropical moisture, and resulting in less rainfall, change in the weathering patterns, and consequent changes in the clay-mineral assemblages of the basin sediments.

The sharp increases in chlorite content and the (Ch+I)/(K+S) ratio, together with rapid decrease in the Kübler index value, suggest that rapid cooling occurred at 8.4 Ma. However, the sharp increase in kaolinite and smectite contents and the decrease in the (Ch+I)/(K+S) ratio and the slightly large Kübler index value suggest that the warming event took place at ~3.6 Ma in the Zhada area since the late Miocene. Global cooling occurred at 8.2 and 3.3 Ma and global warming at ~5.5 Ma (Miller *et al.*, 2005). The cooling at 8.4 Ma in Zhada occurred prior to the corresponding global cooling by 0.2 Ma. No response to the global warming at ~5.5 Ma and to the global cooling at 3.3 Ma was observed in Zhada area. The climatic evolution in Zhada is evidently more influenced by local tectonic uplift than by global climatic trends.

In a recent study of the Zhada section, Kempf *et al*. (2009) showed that significant change in weathering conditions and drainage patterns occurred at 90 m from the base, corresponding to the change at 8.4 Ma observed in the present study. The sediments are characterized by upward coarsening in the upper part of the lithofacies unit of 0−90 m, indicating a strong and

rapid increase in discharge during the period, which was mainly attributed to tectonic activity (Clevis *et al.*, 2004). Subsequent to the tectonic activity, the fluvial plain was inundated rapidly by a lake, as indicated by the retrogradational deltaic depositional sequences. The rapid increase in chlorite content and the subsequent cooling at 8.4 Ma was probably indicative of a sharp local tectonic uplift, as suggested by Tapponnier *et al.* (2001), different stages of growth of the Plateau may contribute to trigger or enhance different climatic effects at different times by shifting atmospheric circulation patterns.

A gradual increase in the value of (Ch+I)/(K+S) was also observed at ~4.5 Ma (Figure 5), in association with the decreasing Kübler index value and the subsequent increase in smectite and kaolinite content. These suggest that a rapid increase in relief was produced in the region during the period, as also indicated by the coarse-grained sediments due to the large increase in sediment supply (Saylor *et al*., 2009), which was considered to be as a result of rapid subsidence of the basin at that time (Saylor *et al*., 2010b).

An increase in the illite and chlorite contents and in the ratio of (Ch+I)/(K+S) occurred at ~3.6 Ma, followed by a sudden increase in smectite and kaolinite abundance and in the detrital material content of quartz and feldspars, as well as a slight increase in the Kübler index value. Again, the sediments of this period are characterized by the very thick and massive gravel beds. All these indicate that the sediments were derived from erosion of surface materials under a sharp increase in relief, and, therefore, indicate a rapid uplift at ~3.6 Ma in the area. The warming climate conditions could probably be interpreted as the temperature increase effect of mountain mass. Rapid uplift at 3.6 Ma was also reported from Gyirong basin in southern Tibet (Shi *et al.*, 1998; Yue *et al.*, 2004; Hong *et al*., 2010) and in many other areas in the Tibetan Plateau (Li and Fang, 1999; Zheng *et al*., 2000; Parés *et al*., 2003).

The near coincidence of environmental change at ~8 Ma in and near the Tibetan Plateau with the tectonic event in the same area has been interpreted as rapid growth of the Tibetan Plateau at or just before ~8 Ma (Harrison *et al*. 1992; Molnar *et al*. 1993). The rise of the Tibetan Plateau during that period resulted in regional climate changes, including a strengthening of the Indian monsoon and intensification of loess deposition at ~7−8 Ma (Rea *et al*., 1998; An *et al.*, 2001). In the Zhada basin, however, the clay indices of the sediments suggest that strong uplift occurred at 8.4 and 3.6 Ma, with rapid subsidence of the basin at 4.5 Ma. The presence of smectite and kaolinite throughout the Zhada sediments suggest that overall warm and probably sub-humid climate conditions prevailed during that period; though some climate change occurred in association with uplift of the Tibetan Plateau, the uplift in southern Tibet was insufficient to prevent entry of tropical moisture from the eastern Pacific Ocean and Indian Ocean and cause aridification, which prevails at present in the Zhada basin, prior to 3.0 Ma.

CONCLUSIONS

Clay indices of the Zhada sequences have indicated that the climate was warm and humid from 9.5 to 8.4 Ma, relatively cool and dry from 8.4 to 7.2 Ma, warm and seasonally arid from 7.2 to 4.5 Ma, cool and humid from 4.5 to 3.6 Ma, and warm and humid from 3.6 to 3.0 Ma. Fluctuations in the Kübler index and in terms of the abundance of the evaporite minerals dolomite, aragonite, and gypsum during the period 7.2−4.5 Ma imply strong climatic fluctuations between humid and seasonal humid conditions in the Zhada basin.

Rapid uplift around the Zhada basin was observed at 8.4 and 3.6 Ma, with sharp subsidence of the basin at 4.5 Ma. The abrupt cooling at 8.4 probably reflects the intense uplift of the Himalayas and its cooling effect (caused by the blockage of tropical moisture), while the abrupt warming at 3.6 Ma suggests the warming effect of the Himalayan uplift (perhaps caused by an inability to shift atmospheric circulation patterns, which may lead to a mountain-warming effect). Climate evolution in Zhada differed from global climatic change and this can be attributed to the local tectonics-led climate change.

ACKNOWLEDGMENTS

The present work was supported by the China Geological Survey (No.1212011121261), the Natural Science Foundation of China (41072030 and 40872038), the Specialized Research Fund for the Doctoral Program of Higher Education of China (20110145110001), and the Open Project Foundation of State Key Laboratory of Geological Processes and Mineral Resources (GPMR200910). The authors thank Y.D. Xu for sample preparation, Dr S.B. Mu for SEM work, J.S. Yu for XRD analyses, and, in particular, Prof. J.W. Stucki, Editor-in-Chief, Prof. S. Kadir, Associate Editor, and Prof. J. Środoń, Prof. F. Nieto, and two anonymous reviewers for their insightful reviews, comments, and suggestions.

REFERENCES

Aitchison, J.C., Ali, J.R., and Davis, A.M. (2007) When and where did India and Asia collided? *Journal of Geophysical Research*, **112**, B05423, 1−19.

An, Z.S., Kutzbach, J.E., Prell, W.L., and Porter, S.C. (2001) Evolution of Asian monsoons and phased uplift of the Himalaya-Tibetan since Late Miocene times. *Nature*, **411**, 62−66.

Anadón, P., Burjachs, F., Martín, M., Rodriguez-Lázaro, J., Robles, F., Utrilla, R., and Vázquez, A. (2002) Paleoenvironmental evolution of the Pliocene Villarroya Lake, northern Spain. A multidisciplinary approach. *Sedimentary Geology*, **148**, 9−27.

Biscaye, P.E. (1965) Mineralogy and sedimentation of recent deep-sea clays in the Atlantic Ocean and adjacent seas and oceans. *Geological Society of America Bulletin*, **76**, 803−832.

Chamley, H. (1989) *Clay Sedimentology*. Springer-Verlag,

Heidelberg, Germany, 623 pp.
Clevis, Q., de Boer, P.L., and Nijman, W. (2004) Differentiating the effect of episodic tectonism and eustatic sea-level fluctuations in foreland basins filled by alluvial fans and axial deltaic systems: insights from a three-dimensional stratigraphic forward model. *Sedimentology*, **51**, 809–835.
Dettman, D.L., Kohn, M.J., Quade, J., Ryerson, F.J., Ojha, T.P., and Hamidullah, S. (2001) Seasonal stable isotope evidence for a strong Asian monsoon throughout the past 10.7 m.y. *Geology*, **29**, 31–34.
Enzel, Y., Ely, L.L., Mishra, S., Ramesh, R., Amit, R., Lazar, B., Rajaguru, S.N., Baker, V.R., and Sadler, A. (1999) High-resolution Holocene environmental changes in the Thar Desert, northwestern India. *Science*, **284**, 125–128.
Fagel, N., Debrabant, P., and André, L. (1994) Clay supplies in the Central Indian Basin since the Late Miocene: climatic or tectonic control? *Marine Geology*, **122**, 151–172.
Fagel, N., Boski, T., Likhoshway, L., and Oberhaensli, H. (2003) Late Quaternary clay mineral record in Central Lake Baikal Academician Ridge, Siberia. *Palaeogeography, Palaeoclimatology, Palaeoecology*, **193**, 159–179.
France-Lanord, C. and Derry, L.A. (1994) $\delta^{13}C$ of organic carbon burial forcing of the growth of the carbon cycle from Himalayan erosion. *Geochimica et Cosmochimica Acta*, **58**, 4809–4814.
Flynn, L.J. and Jacobs, L.L. (1982) Effects of changing environments on Siwalik rodent faunas of northern Pakistan. *Palaeogeography. Palaeoclimateology, Palaeoecology*, **38**, 129–138.
Garzione, C.N., Dettman, D.L., Quade, J., DeCelles, P.G., and Butler, R.F. (2000) High times on the Tibetan Plateau: Paleoelevation of the Thakkhola graben, Nepal. *Geology*, **28**, 339–342.
Garzione, C.N., DeCelles, P.G., Hodkinson, D.G., Ojha, T.P., and Upreti, B.N. (2003) East-west extension and Miocene environmental change in the southern Tibetan plateau: Thakkhola graben, central Nepal. *Geological Society of America Bulletin*, **115**, 3–20.
Gaucher, G. (1981) *Les Facteurs de la Pedogenese*. G. Lelotte, Dison, Belgium, 730 pp.
Grosjean, M., van Leeuwen, J.F.N., van der Knaap, W.O., Geyh, M.A., Ammann, B., Tanner, W., Messerli, B., Nunez, L.A., Valero-Garces, B.L., and Veit H. (2001) A 22,000 ^{14}C year BP sediment and pollen record of climate change from Laguna Miscanti 23ºS, northern Chile. *Global and Planetary Change*, **28**, 35–51.
Hallam, A., Grose, J.A., and Ruffell, A.H. (1991) Paleoclimatic significance of changes in clay mineralogy across the Jurassic-Cretaceous boundary in England and France. *Palaeogeography, Palaeoclimateology, Palaeoecology*, **81**, 173–187.
Harrison, T.M., Copeland, P., Kidd, W.S.F., and Yin, A. (1992) Raising Tibet. *Science*, **255**, 1663–1670.
Hillier, S. (2000) Accurate quantitative analysis of clay and other minerals in sandstones by XRD: comparison of a Rietveld and a reference intensity ratio (RIR) method and the importance of sample sparation. *Clay Minerals*, **35**, 291–302.
Hong, H.L., Li, Z.H., Xue, H.J., Zhu, Y.H., Zhang, K.X., and Xiang, S.Y. (2007) Oligocene clay mineralogy of the Linxia basin: evidence of palaeoclimatic evolution subsequent to the initial-stage uplift of the Tibetan plateau. *Clays and Clay Minerals*, **55**, 492–505.
Hong, H.L., Zhang, K.X., and Li, Z.H. (2010) Climatic and tectonic uplift evolution since ~7 Ma in Gyirong basin, southwestern Tibet plateau: Clay-mineral evidence. *International Journal of Earth Science*, **99**, 1305–1315.
Hoorn, C., Ohja, T., and Quade, J. (2000) Palynological evidence for vegetation development and climatic change in the sub-Himalayan zone (Neogene, Central Nepal). *Palaeoclimatology, Palaeogeography, Palaeoecology*, **163**, 133–161.
Hu, S., Goddu, S.R., Appel, E., Verosub, K., Yang, X., and Wang, S. (2005) Palaeoclimatic changes over the past 1 million years derived from lacustrine sediments of Heqing basin (Yunnan, China). *Quaternary International*, **136**, 123–129.
Huang, C.M. and Wang, C.S. (2001) A review on paleosols and uplift of Qinghai-xizang plateau. *Geological Science and Technology Information*, **20**, 1–4 (in Chinese with English abstract).
Huang, Z.G., Zhang, W.Q., and Chen, J.H. (1999) The change of natural zones and the evolution of red earth in China. *Acta Geographica Sinica*, **54**, 193–203 (in Chinese with English abstract).
Jackson, M.L. (1978) *Soil Chemical Analyses*. Published by the author, University of Wisconsin, Madison, Wisconsin, USA.
Kempf, O., Blisniuk, P.M., Wang, S., Fang, X., Wrozyna, C., and Schwalb, A. (2009) Sedimentology, sedimentary petrology, and paleoecology of the monsoon-driven, fluvio-lacustrine Zhada Basin, SW-Tibet. *Sedimentary Geology*, **222**, 27–41.
Li, J.G. and Zhou, Y. (2001) Pliocene palynoflora from the Zhada basin, west Xizang (Tibet) and the palaeaoenvironment. *Acta Micropalaeontologica Sinica*, **18**, 89–96 (in Chinese with English abstract).
Li, J.J. and Fang, X. (1999) Uplift of the Tibetan Plateau and environmental changes. *Chinese Science Bulletin*, **44**, 2117–2124.
Lindgreen, H. and Surlyk, F. (2000) Upper Permian-Lower Cretaceous clay mineralogy of East Greenland: provenance, paleoclimate and volcanicity. *Clay Minerals*, **35**, 791–806.
Manju, C.S., Narayanan Nair, V., and Lalithambika, M. (2001) Mineralogy, geochemistry and utilization study of the Madayi kaolin deposits, north Kerala, India. *Clays and Clay Minerals*, **49**, 355–369.
Miller, K.G., Kominz, M.A., Browning, J.V., Wright, J.D., Mountain, G.S., Katz, M.E., Sugarman, P.J., Cramer, B.S., Christie-Blick, N., and Pekar, S.F. (2005) The Phanerozoic record of Global Sea-Level Change. *Science*, **310**, 1293–1298.
Millot, G. (1970) *Geology of Clays*. Springer-Verlag, Berlin, 499 pp.
Molnar, P., England, P., and Martinod, J. (1993) Mantle dynamics, the uplift of the Tibetan Plateau, and the Indian monsoon. *Reviews of Geophysics*, **31**, 357–396.
Murphy, M.A., Yin, A., Kapp, P., Harrison, T.M., Manning, C.E., Ryerson, F.J., Ding, L., and Guo, J. (2002) Structural evolution of the Gurla Mandhata detachment system, southwest Tibet: implications for the eastward extent of the Karakoram fault. *Geological Society of America Bulletin*, **114**, 428–447.
Ojha, T.P., Butler, R.F., Quade, J., DeCelles, P.G., Richards, D., and Upreti, B.N. (2000) Magnetic polarity stratigraphy of the Neogene Siwalik Group at Khutia Khola, far western Nepal. *Geological Society of America Bulletin*, **112**, 424–434.
Parés, J.M., Van der Voo, R., Downs, R.W., Yan, M., and Fang, X. (2003) Northeastward growth and uplift of the Tibetan Plateau: Magnetostratigraphic insights from the Guide Basin. *Journal of Geophysical Research*, **108**, 1–11.
Perry, E.A. and Hower, J. (1970) Burial diagenesis in Gulf Coast politic sediments. *Clays and Clay Minerals*, **18**, 165–177.
Qian, F. (1999) Study on magnetostratigraphy in Qinghai–Tibetan Plateau in late Cenozoic. *Journal of Geomechanics*, **5**, 22–34 (in Chinese text with English abstract).

Quade, J., Cater, J., Ojha, T., Adam, J., and Harrison, T. (1995) Late Miocene environmental change in Nepal and the northern Indian subcontinent: Stable isotopic evidence from paleosols. *Geological Society of America Bulletin*, **107**, 1381–1397.

Rea, D.K., Snoeckx, H., and Joseph, L.H. (1998) Late Cenozoic eolian deposition in the North Pacific: Asian drying, Tibetan uplift, and cooling of the northern hemisphere. *Paleoceanography*, **13**, 215–224.

Saylor, J.E., Quade, J., Dellman, D.L., DeCelles, P.G., Kapp, P.A., and Ding, L. (2009) The late Miocene through present paleoelevation history of southwestern Tibet. *American Journal of Science*, **309**, 1–42.

Saylor, J., DeCelles, P., and Quade, J. (2010a) Climate-driven environmental change in the Zhada basin, southwestern Tibetan Plateau. *Geosphere*, **6**, 74–92.

Saylor, J., DeCelles, P., Gehrels, G., Murphy, M., Zhang, R., and Kapp, P. (2010b) Basin formation in the High Himalaya by arcparallel extension and tectonic damming: Zhada basin, southwestern Tibet. *Tectonics*, **29**, TC1004, doi:10.1029/2008TC002390.

Schieber, J. (1986) Stratigraphic control of rare-earth pattern types in mid-Proterozoic sediments of the Belt Super Group, Montana, U.S.A.: implications for basin analysis. *Chemical Geology*, **54**, 135–148.

Shi, Y.F., Li, J.J., and Li, B.Y. (1998) *Late Cenozoic Uplift and Environmental Change of Qinghai-Tibet Plateau*. Guangdong Science & Technology Press, Guangzhou, China 463 pp. (in Chinese).

Singer, A. (1984) The paleoclimatic interpretation of clay minerals in sediments – a review. *Earth Science Reviews*, **21**, 251–293.

Solotchina, E.P., Prokopenko, A.A., Kuzmin, M.I., Solotchin, P.A., and Zhdanova, A.N. (2009) Climate signals in sediment mineralogy of Lake Baikal and Lake Hovsgol during the LGM-Holocene transition and the 1-Ma carbonate record from the HDP-04 drill core. *Quaternary International*, **205**, 38–52.

Tapponnier, P., Xu, Z., Roger, F., Meyer, B., Arnaud, N., Wittlinger, G., and Yang, J. (2001) Oblique stepwise rise and growth of the Tibet Plateau. *Science*, **294**, 1671–1677.

Thiede, R.C., Arrowsmith, J.R., Bookhagen, B., McWilliams, M.O., Sobel, E.R., and Strecker, M.R. (2006) Dome formation and extension in the Tethyan Himalaya, Leo Pargil, northwest India. *Geological Society of America Bulletin*, **118**, 635–650.

Thiry, M., (2000) Palaeoclimatic interpretation of clay minerals in marine deposits: an outlook from the continental origin. *Earth-Science Reviews*, **49**, 201–221.

Van Lith, Y., Warthmann, R., Vasconcelos, G., and McKenzie, J.A. (2003) Sulphate reducing bacteria induce low-temperature Ca-dolomite and high Mg-calcite formation. *Geobiology*, **1**, 71–79.

Wang, S., Zhang, W., Fang, X., Dai, S., and Kempf, O. (2008) Magnetostratigraphy of the Zanda basin in southwest Tibet Plateau and its tectonic implications. *Chinese Science Bulletin*, **53**, 1393–1400.

Wang, Y., Deng, T., and Biasatti, D. (2006) Ancient diets indicate significant uplift of southern Tibet after ca. 7 Ma. *Geology*, **34**, 309–312.

Weaver, C.E. (1989) *Clays, Muds, and Shales*. Developments in Sedimentology, **44**, Elsevier, Amsterdam, 819 pp.

Yue, L.P, Deng, T., Zhang, R., Zhang, Z.Y., Heller, F., Wang, J.Q., and Yang, L.R. (2004) Paleomagnetic chronology and records of Himalayan uplift on the Longgugou section of Gyirong-Oma basin, Tibet. *Chinese Journal of Geophysics*, **47**, 1009–1016 (in Chinese with English abstract).

Zhang, K.X., Wang, G.C., Cao, K., Liu, C., Xiang, S.Y., Hong, H.L., Kou, X.H., Xu, Y.D., Chen, F.N., Meng, Y.N., and Chen, R.M. (2008) Cenozoic sedimentary records and geochronological constraints of differential uplift of the Qinghai-Tibet Plateau. *Science in China Series D: Earth Sciences*, **51**, 1658–1672.

Zheng, H., Powell, C.M., An, Z., Zhou, J., and Dong, G. (2000) Pliocene uplift of the northern Tibetan Plateau. *Geology*, **28**, 715–718.

Zhu, D.G., Meng, X.G., Shao, Z.G., Yang, C.B., Han, J.E., Yu, J., Meng, Q.W., and Lu, R.P. (2007) Evolution of the paleovegetation, paleoenvironment and paleoclimate during Pliocene-early Pleistocene in Zhada Basin, Ali, Tibet. *Acta Geologica Sinica*, **81**, 295–306 (in Chinese with English abstract).

(*Received 4 August 2011; revised 6 April 2012; Ms. 599; A.E. S. Kadir*)